Earth Planets Space, **54**, 81–89, 2002

Spatial and temporal characteristics of low-magnitude seismicity from a dense array in western Nagano Prefecture, Japan

Paul A. Rydelek[1], Shigeki Horiuchi[2], and Yoshihisa Iio[3]

[1]*Center for Earthquake Research and Information, The University of Memphis, Memphis, TN 38152, U.S.A.*
[2]*National Research Institute for Earth Science and Disaster Prevention, Science and Technology Agency, Ibaraki 305-0006, Japan*
[3]*Earthquake Research Institute, University of Tokyo, 1-1-1 Yayoi, Bunkyo, Tokyo 113-0032, Japan*

(Received October 30, 2000; Revised June 28, 2001; Accepted August 4, 2001)

We analyze an earthquake catalog and waveform data from a dense seismic array in western Nagano Prefecture in order to investigate seismic properties and source parameters. The catalog used here consists of about 30,000 smaller magnitude earthquakes that were located within a source volume of order (10 km)^3. Moving window analysis shows that the seismic rate is steady over time and the temporal change in the size distribution of earthquakes shows only statistical fluctuations. Spatial analyses, however, reveals that certain features of seismicity are depth-dependent. At shallow depths (<3 km), we find an increase in average stress drop with depth that may be related to the characteristic depth of seismicity (the depth where the frequency of earthquakes is maximum). The b-value is also found to be elevated throughout depths where the seismicity is most intense but then the b-value slowly decreases as depth increases. Another result from our analysis of waveform data is a clear relation between earthquake magnitude and stress-drop in the magnitude range -0.5 to 2.5.

1. Introduction

The Ootaki seismic array is located in the western part of Nagano prefecture near the base of Mt. Ontake volcano in central Japan (see Fig. 1). This region is known to be seismically active since monitoring began in 1976 and these early seismic observations revealed intervals of intense earthquake clustering in several localized areas (Seismic Activity Monitoring Center, 1977). These bursts of seismic activity evidently preceded an unusual steam eruption of Mt. Ontake in 1979 (Aoki *et al.*, 1980); prior to this short-lived eruption there is no historical record of volcanic activity on Mt. Ontake. In 1984, five years after the eruption and only 9 km from the volcano, a damaging shallow M 6.8 earthquake struck this area (Fig. 1), which has been the subject of much research (see e.g. Ooida *et al.*, 1989; Inamori *et al.*, 1992; Iio and Yoshioka, 1992). The Western Nagano Prefecture Earthquake was unexpected since this area had previously shown only low magnitude seismic activity and seismic clusters of the type more commonly found in volcanic regions. The tectonic implications regarding the volcanic eruption and the major earthquake relatively soon thereafter is still under investigation; this area of Japan has been the focus of increased monitoring with a large number of stations in a fairly small region (Fig. 1), henceforth referred to as the Ootaki array.

The microseismic array at Ootaki is equipped with seismometers and recorders designed to provide high spatial and temporal resolution in the aftershock zone of the 1984 Western Nagano Prefecture Earthquake. The 3-component seismometers are conventional moving-coil velocity transducers (L-22D) but outfitted with a special recording system (EDR6600) that has a flat response for ground velocity up to 4 kHz and with a high-speed sampling frequency of 10 kHz. The analog signal is amplified by different gains and then converted with a 16-bit A/D and stored digitally on removable hard disk that is replaced every several weeks. The average background noise levels of the stations are estimated to be in the range 10^{-7} to 10^{-8} m/s. Station power is obtained from batteries since nearly all of the array sites are located in remote areas that greatly helps to minimize the background noise levels but unfortunately precludes the operation of certain sites during the winter season. In order to precisely time the seismic signals, the system clock is adjusted to a GPS clock every two hours to maintain a system timing accuracy to within 1 ms. The Ootaki array has grown from the initial 6 stations in the summer of 1995 to about 48 stations at the end of 2000 with an inter-station spacing of only a few kilometers. There are also two borehole seismic stations at Ootaki; OT01 and OT02 are located 3 km apart and with depths of 145 m and 100 m, respectively.

2. Data and Analysis

Map and cross sectional views of the hypocenters of the earthquakes recorded by the Ootaki array are shown in Fig. 1. Also shown are the station locations and the section of the fault that ruptured during the 1984 Western Nagano Prefecture M 6.8 Earthquake as determined by Yoshida and Koketsu (1990) from a simultaneous inversion of seismic waveform and geodetic data. Event locations were obtained by using an automatic processing system developed

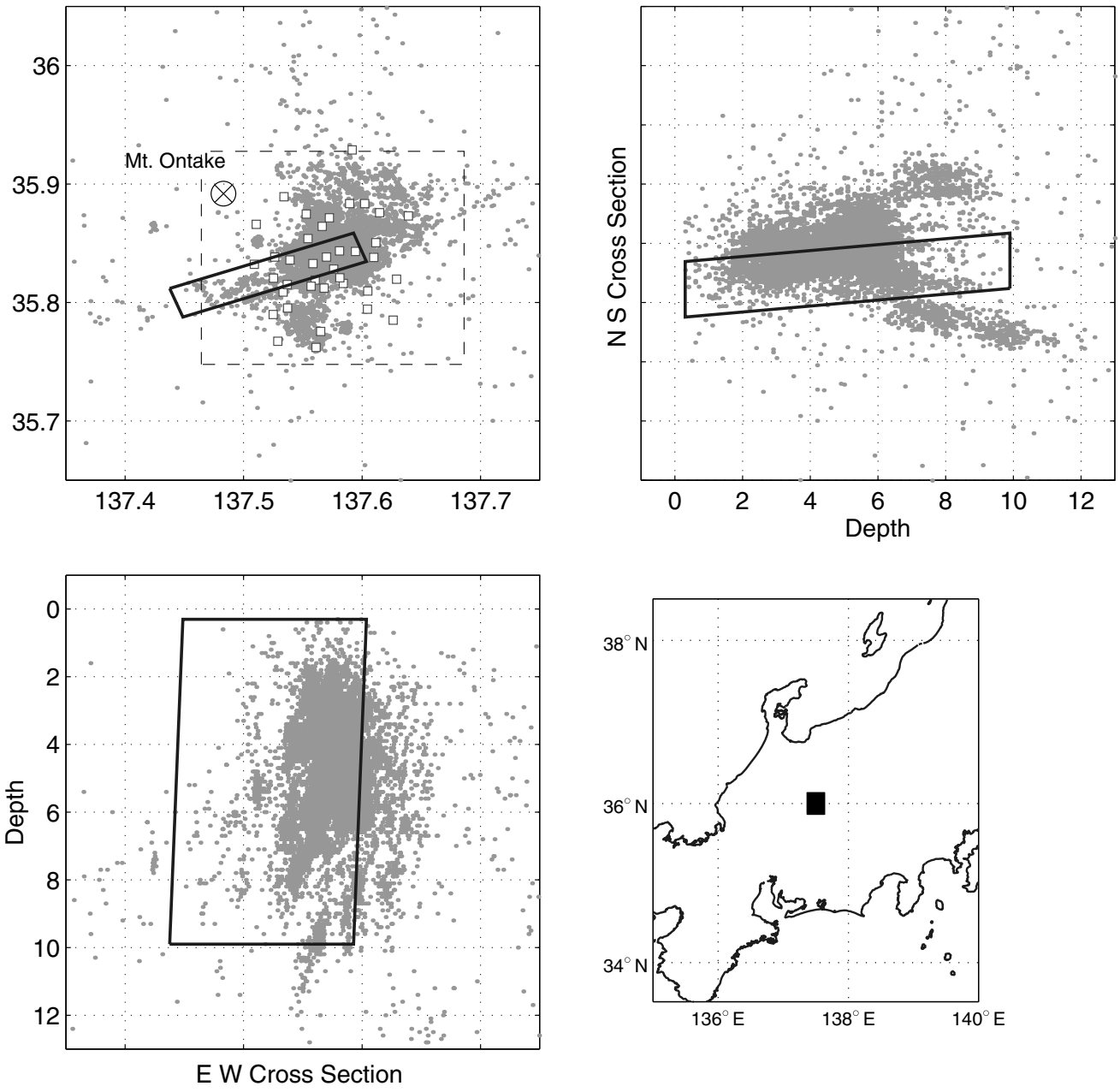

Fig. 1. Map view and cross sectional views showing the distribution of earthquake hypocenters located by the Ootaki array (squares) from late May 1995 to mid October 1999. The rectangle is the fault plane of the 1984 Western Nagano Prefecture M 6.8 Earthquake. The dashed box in the map view to a depth of 10 km contains the bulk of the seismicity used in our analysis.

by Horiuchi *et al.* (1999). In order to allow for lateral heterogeneity in earth structure and especially at shallow depths, the station corrections and hypocenters were determined simultaneously for all events. Evidence of the high quality of the seismic data recorded at Ootaki array is found in the P-wave rms travel time residuals that are smaller than 0.01 s for about 80% of the earthquake catalog. The bulk of the seismicity at Ootaki is confined to an area of roughly 10 km $\times$ 10 km and to depths shallower than about 10 km.

The detection level of the Ootaki array can be simply estimated by plotting the cumulative number of events versus time as shown in Fig. 2. Clearly, small earthquakes with magnitudes $\sim$1 or less are not always detected since changes in the rate of these events apparently coincides with changes in the number of stations comprising the Ootaki array, i.e. more of these smaller events are recorded as the number of stations increases, most revealing in the early years of operation. Above some magnitude level, however, events are recorded at a rate that is independent of the increase in the number of stations and this magnitude level at Ootaki is about 1.5; after several years of station deployment this level is probably much lower. This paper is not intended to investigate the completeness level of the Ootaki array, so we therefore restrict our analysis, except when noted, to events with magnitudes $M \geq 1.5$. The curve in Fig. 2 for these events reveals no significant correlation with

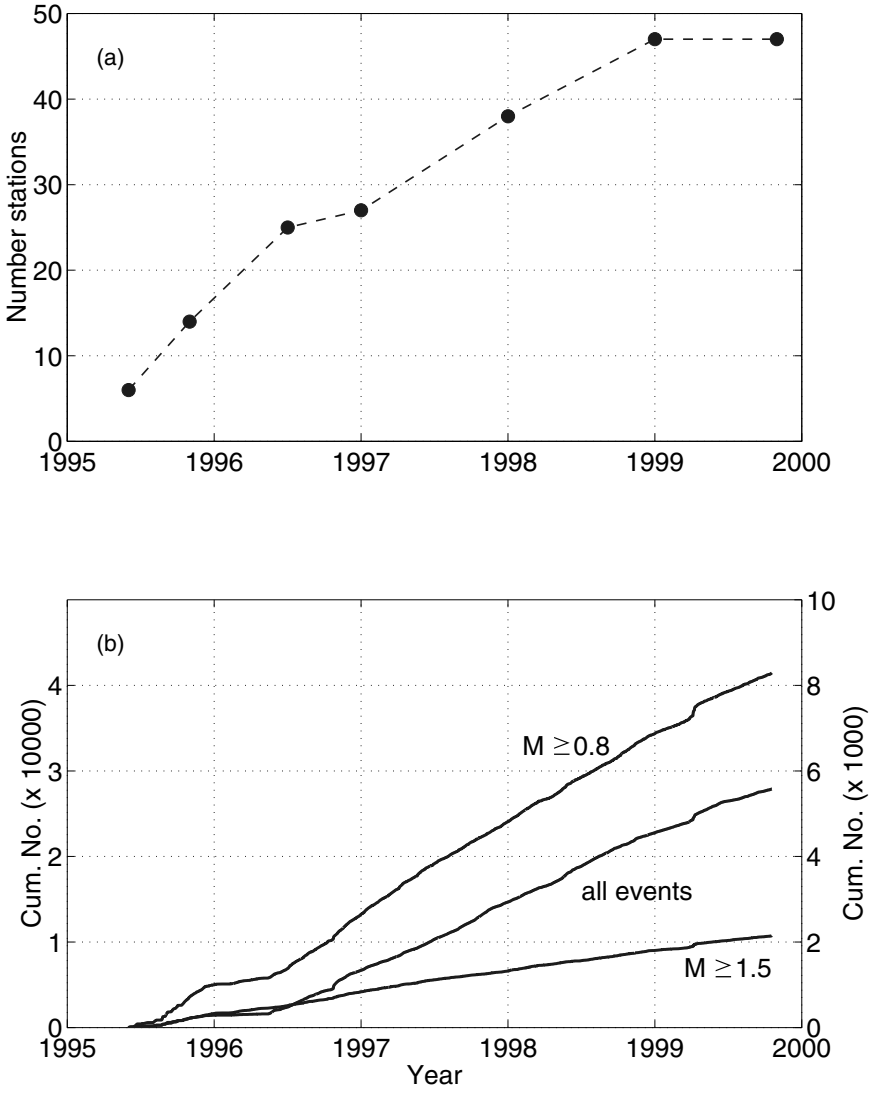

Fig. 2. (a) Plot of the number of seismic stations at Ootaki versus time. These numbers do not include the closing of certain stations during the winter season. (b) Plot of the cumulative number of seismic events versus time. The middle curve for all events uses the left hand scale, while the other two curves use the right hand scale; the right hand scale is a factor of 5 smaller than the left hand scale.

the change in the number of stations even when the ordinate scale is greatly amplified. Additional evidence for a complete catalog at least for $M \geq 1.5$ earthquakes comes from the catalog completeness test developed by Rydelek and Sacks (1989). Although this method of testing catalog completeness has been questioned when used on seismic catalogs with a spatial variation in completeness (see e.g. Gomberg, 1991; Wiemer and Wyss, 2000) it is nevertheless an easy statistical test to apply and can expose temporal variations in seismicity not found by other tests of completeness (Rydelek and Sacks, 1992). Given the relatively small seismic region studied here and the density of stations covering this area, a significant spatial variation in completeness at Ootaki is not expected. Therefore, we tested both the early (six stations) and late (full array) portions of the Ootaki catalog using the Rydelek and Sacks method and found no significant diurnal modulation of the seismicity when events with magnitudes $\geq$1.5 were used. When present, this modulation is produced by small events just at the detection level of the array, since more of these events are recorded during the night when ambient noise levels are lower than during the day, thus resulting in a 24-hour periodicity in seismicity. Indeed, the Ootaki catalog showed the presence of a annual modulation of seismicity when events of all magnitudes were used and this is presumably caused by the closing of certain stations during the winter season mentioned previously. Faced with the dilemma of using many smaller events that are accurately located but may sometimes be missed and could therefore raise questions regarding our results, we have restricted our analysis to only $M \geq 1.5$ earthquakes, except where noted. We have also restricted our analysis to those events shallower than 10 km so as to avoid any problems with catalog completeness as a function of depth. To lend further support to the completeness level of the Ootaki catalog, Fig. 3 shows a plot of the seismograms from 16 randomly selected stations of a small $M = 1.5$ event that occurred in October 1998 near the deepest level (=10 km) in our analyses; clearly, events of this size in our study area

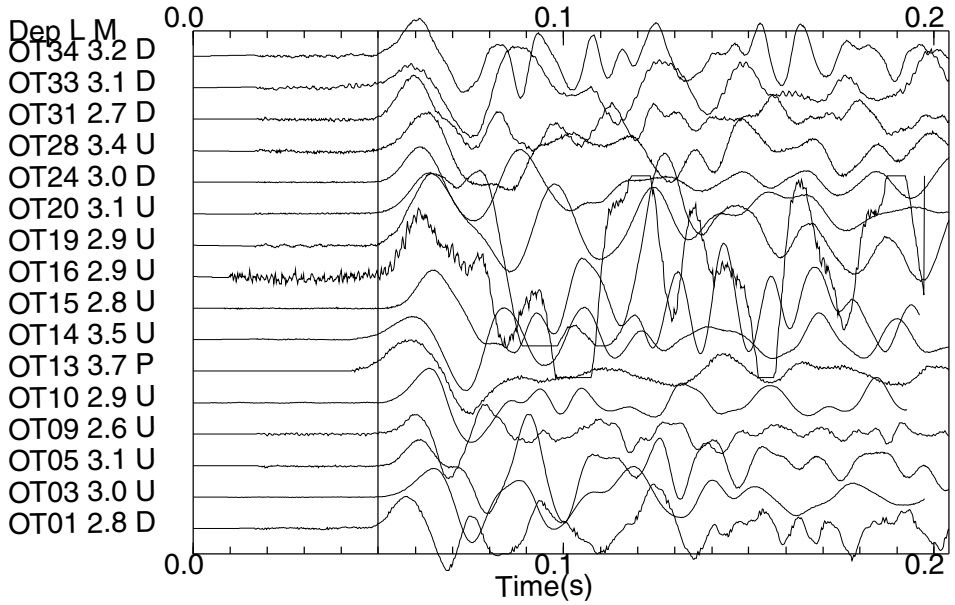

Fig. 3. Detection capability of the Ootaki array as evidenced by seismograms from 16 randomly selected stations of a small $M = 1.5$ earthquake located at the deepest level ($\sim$10 km) in our analysis. This figure also demonstrates the accuracy of the automatic P picker.

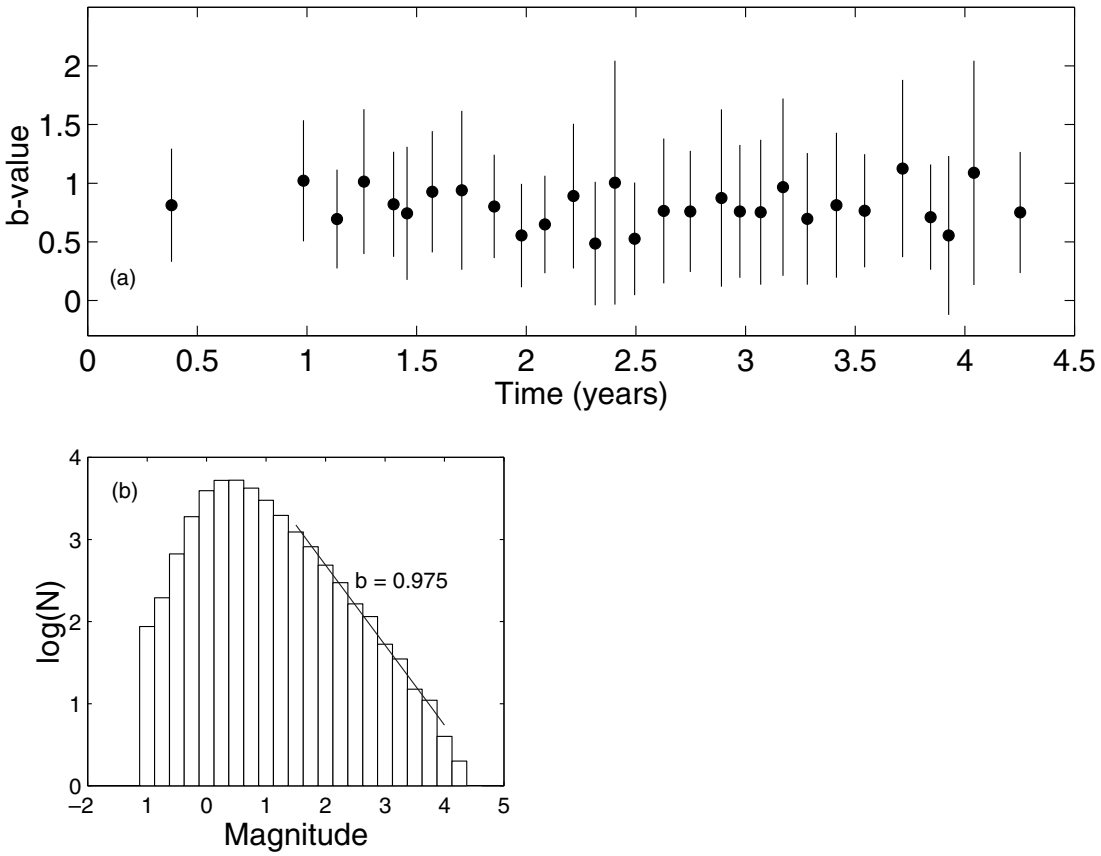

Fig. 4. (a) Temporal estimates of b-value from a moving window analysis of the Ootaki catalog. Each window consists of 1000 earthquakes (roughly 2 months using the full array) but only events with $M \geq 1.5$ were used in estimating the b-value. Vertical lines for each estimate are error bars ± 1 standard deviation. Notice the increased detection of small events as the number of stations increased significantly after the first year. (b) Frequency distribution of earthquake magnitudes for the entire catalog.

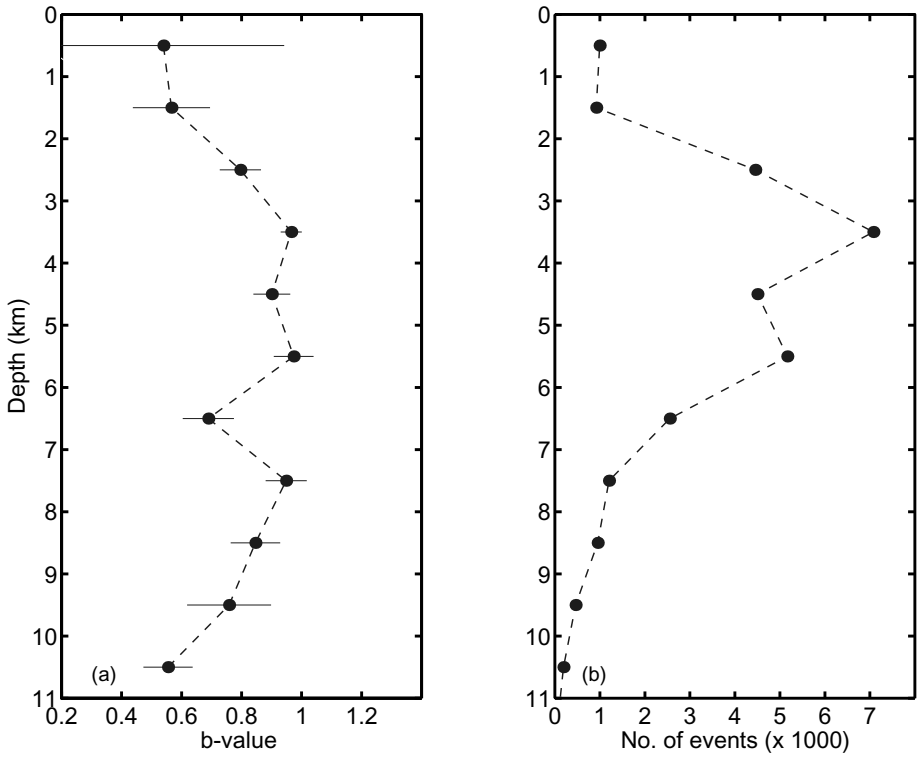

Fig. 5. (a) Dependence on b-value with depth. Estimates are for earthquakes with $M \geq 1.5$ within 1 km depth intervals. Horizontal lines are error bars ± 1 standard deviation. (b) The number of earthquakes as a function of depth.

are recorded with excellent S/N throughout the Ootaki array. More sophisticated tests of determining the completeness level would enable future studies to use much more of the catalog (i.e. smaller magnitude events) to investigate the seismicity at Ootaki.

The distribution of earthquake sizes (or b-value) for the entire catalog is shown Fig. 4. Again we see that for earthquakes with $M \geq 1.5$ the catalog may appear complete as suggested by the linearity of the b-value curve above this magnitude level; this of course presupposes that the distribution of events in a complete catalog will follow a linear b-value curve. The earthquake catalog was analyzed by the method of a moving time window to determine if there were any significant long-term changes in the distribution of earthquake sizes, or b-value, in the catalog. The b-value was estimated by fitting a least squares line to the distribution of the frequency of earthquakes with magnitudes ≥ 1.5 (e.g. see Fig. 4(b)). The establishment of baseline observations at Ootaki may prove to be important in earthquake prediction research, since anomalous changes in such baseline readings might be used as a precursory warning signal before a large damaging earthquake. Figure 4(a) shows the b-values that were estimated from a moving window analysis that contained 1000 earthquakes in each (independent) window. Within the statistical uncertainties, each estimate is close to the b-value of the full catalog (Fig. 4(b)) and no significant changes can be observed during the $\sim$5 years the catalog was recorded.

Because of the density and quality of the stations at Ootaki, and combined with the high rate of seismicity, the earthquake source parameters can be accurately estimated and the spatial dependence of the seismicity can be investigated with high depth resolution. The depth distribution of the seismicity is shown in Fig. 5(b) where the number of earthquakes from the central part of the array (see Fig. 1) is plotted in 1 km depth intervals. We also placed an additional restriction on these events such that only well located events with P-wave rms residuals ≤ 0.05 s were used. The characteristic depth of seismicity is found to be from 3–4 km; recall that the characteristic depth is defined at the depth of maximum seismicity; variations in this depth are expected since this depth reflects regional differences in crustal structure and tectonic environment. The b-value as a function of depth, and computed using only events with $M \geq 1.5$, is also shown in Fig. 5. Although there may be some suggestion of a maximum in the b-value at the characteristic depth of seismicity, the overall curve looks mostly flat at intermediate depths (4–8 km) and then gradually rolls off at greater depths. However, there appears to be an anomalously low b-value in the depth range 0–3 km, albeit with a large uncertainty at the shallowest depth; this depth range also shows the smallest average stress drop as discussed below.

In addition to accurate locations from analysis of P-wave arrival times from the array stations, fault parameters consisting of fault size, average slip, and stress drop were estimated from spectral analysis of the P-waves recorded at the borehole station OT01 (see Horiuchi and Iio, 2001). Following the theoretical development of Sato and Hirasawa (1973), we assume that the source spectrum can be modeled as known functions of seismic moment and corner fre-

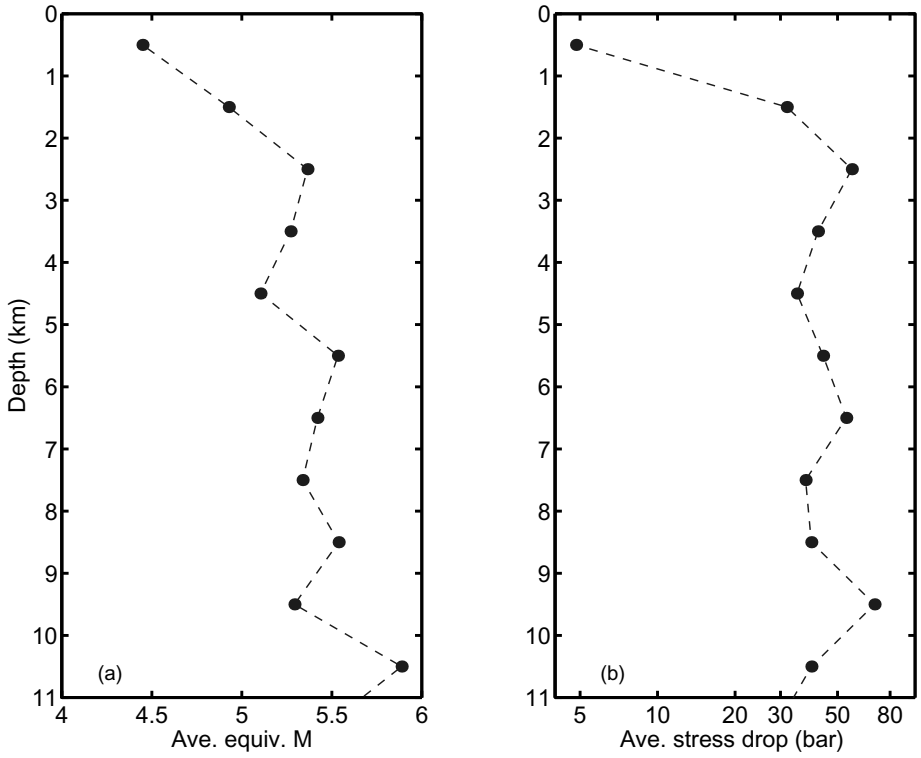

Fig. 6. (a) Plot of average equivalent magnitude versus depth for events with $M \geq 1.5$. (b) Plot of the average stress drop versus depth. Estimates in (a) and (b) are from averages over 1 km depth intervals.

quency. Since seismic waves, however, are affected both by attenuation from inelastic effects and by site effects, the observed spectrum is a complicated function of frequency that is difficult to estimate directly without detailed information about the density and velocity structure at shallow depths; instead, these effects were dealt with in the following manner. A constant attenuation factor with $Q = 300$ was used, and site effects were estimated from an average background spectrum that was determined from all events recorded at the borehole station. In other words, the individual P-wave spectra were fit with fault parameters (i.e. moment and corner frequency) that were earthquake dependent, but also included in the fit was a background spectra (i.e. attenuation and site response) that was assumed to be the same function of frequency for all events (see Horiuchi and Iio, 2001). This model was fit to the observed P-wave spectra by an iterative least squares method, which resulted in a set of χ^2 residuals in parameter space that were used to estimate the uncertainty in model parameters as described below.

Figure 6 shows earthquake stress drops that were obtained from P-wave spectral analysis of well located earthquakes (P-wave rms $\leq$0.05 s) and then spatially averaged over 1 km depth intervals. Figure 6 also shows the average equivalent magnitude that was calculated by finding the total energy of $M \geq 1.5$ events in this depth interval, forming the average energy per earthquake, and then converting this average energy back into an equivalent earthquake magnitude. A relation between the equivalent magnitude and the average stress drop is suggested by the rapid increase in these properties in the depth range 0–3 km.

This relation can be more clearly seen in Fig. 7, which shows a plot of estimated stress drop versus earthquake magnitude for over 17,000 events, regardless of depth. In Fig. 7, catalog completeness is not an issue because all events having P-wave spectra suitable for estimating seismic stress drop can be used. Since stress drop is a function of the corner frequency cubed, errors in the estimation of corner frequency from modeling the P-wave spectra could drastically affect our estimates of stress drop. Therefore, we decided to investigate to what degree errors in parameter estimation might influence the result shown in Fig. 7. The minimum value of the χ^2 residuals in our spectral modeling occurs at the least squares estimates of model parameters and departures from this minimum can be used to estimate parameter uncertainty according to a formula based on the F-statistic (see Jenkins and Watts, 1968, p. 138),

$$\chi^2 \leq \chi_0^2 \left[1 + \frac{k}{N-k} F_{k,N-k}(1-\alpha) \right]$$

where in our case $k = 2$ is the number of source parameters, $N = 66$ is the number of spectral frequencies, and $(1 - \alpha) = 0.68$ provides a confidence level of 1σ; using these values results in the level $\chi^2_{1\sigma} = \chi^2_0[1.0362]$. The minimum value χ^2_0 was used to estimate the corner frequency from which the seismic stress drop was calculated. A parabolic fit was used to interpolate the χ^2 residuals about χ^2_0 in order to find the corner frequencies that corresponded to $\chi^2_{1\sigma}$. These frequencies were then converted to equivalent stress drop, thus providing a measure of the statistical uncertainty in stress drop estimated from the χ^2 distribution. A subset of Fig. 7 is shown in Fig. 8 where the stress

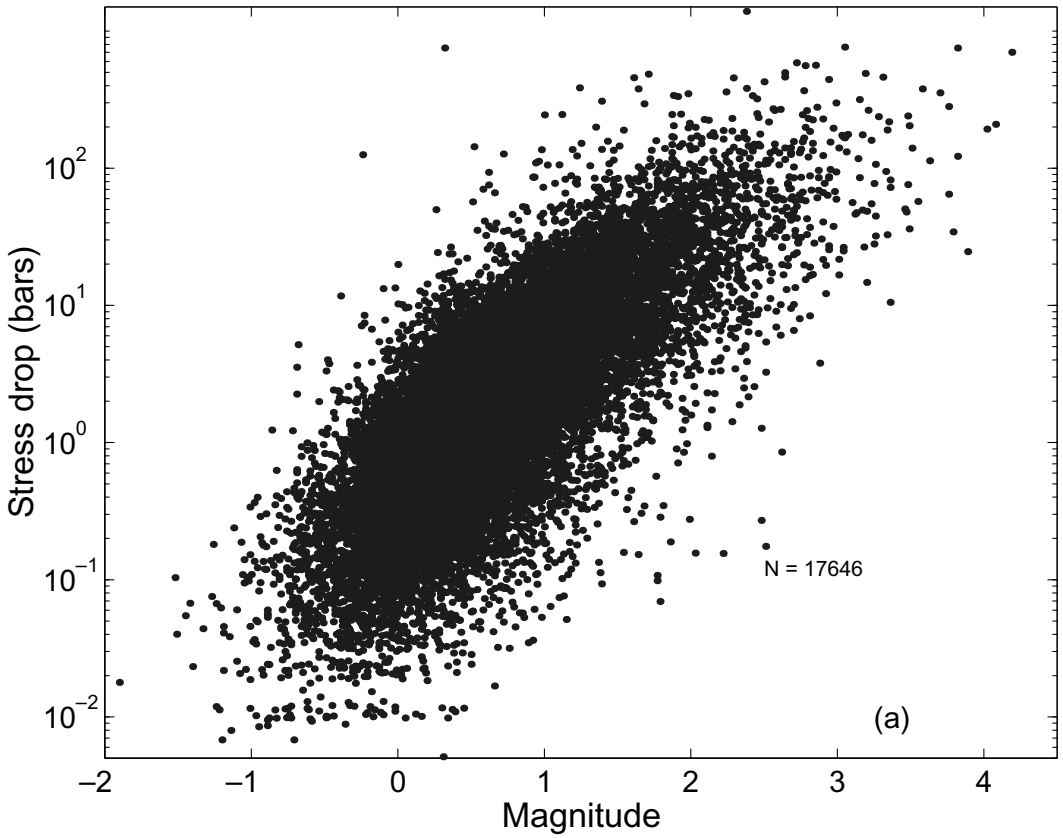

Fig. 7. Plot of stress drop versus magnitude for many well located events that shows a strong linear relation for smaller magnitude earthquakes. Above magnitude ∼2.5 the trend is not clear, albeit the sample size is much smaller.

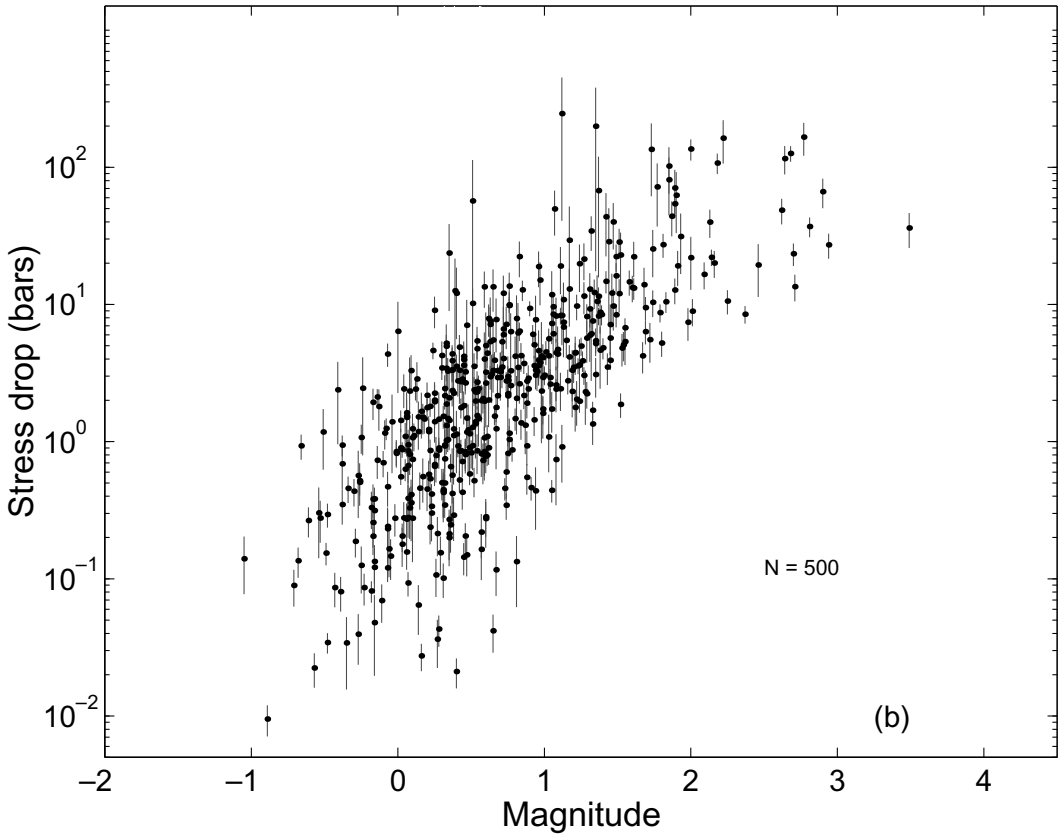

Fig. 8. A subset of 500 randomly selected events in Fig. 7 plotted with error bars ±1 standard deviation.

drops from 500 randomly selected events have been replotted along with their uncertainties as determined by the above method. The main conclusion is unchanged—indeed more strongly supported—namely that stress drop is related to magnitude for the smallest events up to a magnitude level of about 2, at which point the curve seems to level out, suggesting that for larger magnitudes the average stress drop may be relatively constant.

3. Discussion

We have shown that a dense seismic array can be used to investigate the temporal and spatial properties of seismicity within an active seismic zone. In particular, we found the following features in the data from the Ootaki array: no statistically significant changes in the b-value were indicated from a moving window analysis of the seismic catalog; average stress drop increases with depth to about 3 km followed by a very gradual increase at greater depths up to at least 10 km; the b-value increased with depth up to ∼4 km and then was fairly constant over shallow depths (4–8 km) but then decreased with greater depths; the stress drop is strongly correlated with earthquake magnitude for smaller events ($M \leq 2.5$) at any depth.

A spatial variation in stress drop at shallow depths was previously found by Horiuchi and Iio (2001), which was correlated with magnetotelluric measurements of conductivity across the Ootaki fault zone; low stress drop earthquakes were mostly found in regions of low resistivity (Iio *et al*., 2000). The lower resistivity is believed to be related to regions with higher water content that can lead to increased pore pressure across faults, which in turn will affect the confining pressure mentioned below.

Mori and Abercrombie (1997) investigated the depth dependence of seismicity in California and found a systematic decrease in b-value with increasing depth of earthquakes, which they suggested was due to a decrease in heterogeneity and an increase in lithospheric stress with depth. They concluded that their observations were consistent with earthquake models in which earthquake size is undetermined when rupture initiates but the final size is controlled by model properties that stop the rupture. One such model is the non-fractal earthquake model originally developed by Sacks and Rydelek (1995) to explain seismic observations from Matsushiro, Japan (see Dysart *et al*., 1988). This model is one of the general class of cellular automata models based on fundamental physics in which cells fail when a critical Coulomb stress is reached, followed by stress redistribution among neighboring cells after failure. This model is fundamentally different from fractal, or self-similar, earthquake models because fractal models have no inherent lower limit on fault size, whereas the model of Sacks and Rydelek has an explicit assumption of minimum fault (cell) size, typically ∼100 m, which may be related to the scale of heterogeneity at shallow depths. Since fractal models have no size scale, the slip on a fault presumably scales as fault size and therefore stress drop is expected to be mainly constant, independent of earthquake magnitude; this property is universally observed for larger magnitude events. In the cellular earthquake model, however, the smallest fault size is limited and therefore smaller magnitude earthquakes do not imply smaller fault size; instead the stress drop must vary accordingly, which leads to the expectation of stress drop related to earthquake magnitude for smaller events. As cell interaction becomes prevalent in the generation of larger events, then fault size will essentially increase and this model predicts a transition from a regime controlled by stress drop to one controlled by fault size. In computer simulations, the model of Sacks and Rydelek indicated that stress drop will be related to magnitude for small ($M < 3$) earthquakes, as observed (see Fig. 6), but that stress drops will tend to be constant for larger magnitude events. The model also predicts a distribution of earthquake sizes that is dependent on the confining pressure (or depth) of the fault. In short, as the confining pressure is increased, the b-value is expected to decrease and the average earthquake magnitude is expected to increase, which is consistent with the characteristics of the seismicity from the Ootaki array, as well as the California observations noted above.

Acknowledgments. This research was supported by a grant from the Japan Foundation and NSF grant EAR-0003438 that allowed PAR to work at the National Research Institute for Earth Science and Disaster Prevention in Tsukuba, Japan. The friendship and hospitality experienced in Japan is greatly appreciated. CERI contribution 421.

References

Aoki, H., T. Ooida, I. Fujii, and F. Yamazaki, Seismological study of the 1979 eruption of Ontake Volcano, in *Investigation of Volcanic Activity and Disasters Caused by the 1979 Eruption of Ontake Volcano*, edited by H. Aoki, pp. 55–74, Nagoya, Nagoya University, 1980 (in Japanese).

Dysart, P. S., J. A. Snoke, and I. S. Sacks, Source parameters and scaling relations for small earthquakes in the Matsushiro region, southwest Honshu, Japan, *Bull. Seismol. Soc. Am.*, **78**, 571–589, 1988.

Gomberg, J., Seismicity and detection/location threshold in the Southern Great Basin Seismic Network, *J. Geophys. Res.*, **96**, 16401–16414, 1991.

Horiuchi, S. and Y. Iio, Stress drop distribution of micro-earthquakes at Ootaki, Nagano Prefecture, Japan, obtained from waveform data by borehole stations, in *Seismotectonics at the Convergent Zone*, edited by Y. Fujinawa and A. Yoshida, Tokyo, Terra Scientific, 2001.

Horiuchi, S., T. Matsuzawa, and A. Hasegawa, Automatic data processing system of seismic waves that works even at times of huge seismic activity, *J. Seismol. Soc. Japan*, **52**, 241–254, 1999.

Iio, Y. and K. Yoshioka, Strong ground motion in the source region of the 1984 Western Nagano Prefecture Earthquake, inferred from displaced boulders, *J. Phys. Earth*, **40**, 407–419, 1992.

Iio, Y., K. Ikeda, K. Omura, Y. Matsuda, Y. Shiokawa, M. Takeda, and D. Uehara, Conductivity structure of a seismogenic region in the western Nagano prefecture, *Butsuri-tansa*, **53**, 56–66, 2000.

Inamori, T., S. Horiuchi, and A. Hasegawa, Location of mid-crustal reflectors by a reflection method using aftershock waveform data in the focal area of the 1984 Western Nagano Prefecture Earthquake, *J. Phys. Earth*, **40**, 379–393, 1992.

Jenkins, G. M. and D. G. Watts, *Spectral Analysis and Its Applications*, San Francisco, Holden-Day, 1968.

Mori, J. and R. E. Abercrombie, Depth dependence of earthquake frequency-magnitude distributions in California: implications for rupture initiation, *J. Geophys. Res.*, **102**, 15081–15090, 1997.

Ooida, T., F. Yamazaki, and I. Fujii, Aftershock activity of the 1984 Western Nagano Prefecture Earthquake, Central Japan, and its relation to earthquake swarms, *J. Phys. Earth*, **37**, 401–416, 1989.

Rydelek, P. A. and I. S. Sacks, Testing the completeness of earthquake catalogues and the hypothesis of self-similarity, *Nature*, **337**, 251–253, 1989.

Rydelek, P. A. and I. S. Sacks, Comment on "Seismicity and detection/location threshold in the Southern Great Basin seismic network" by Joan Gomberg, *J. Geophys. Res.*, **97**, 15361–15362, 1992.

Sacks, I. S. and P. A. Rydelek, Earthquake 'quanta' as an explanation for observed magnitudes and stress-drops, *Bull. Seismol. Soc. Am.*, **85**, 808–813, 1995.

Sato, T. and T. Hirasawa, Body wave spectrum from propagating shear cracks, *J. Phys. Earth*, **21**, 415–431, 1973.

Seismic Activity Monitoring Center, Seismological Division, J.M.A., Local earthquake at the Kiso district, *Rep. Coord. Comm. Earthq. Predict.*, **17**, 78–79, 1977 (in Japanese).

Wiemer, S. and M. Wyss, Minimum magnitude of completeness in earthquake catalogs: examples from Alaska, the western United States, and Japan, *Bull. Seismol. Soc. Am.*, **90**, 859–869, 2000.

Yoshida, S. and K. Koketsu, Simultaneous inversion of waveform and geodetic data for the rupture process of the 1984 Naganoken-Seibu, Japan, earthquake, *Geophys. J. Int.*, **103**, 355–362, 1990.

P. A. Rydelek (e-mail: par@ceri.menphis.edu), S. Horiuchi, and Y. Iio